

Numerical study of the one-dimensional quantum compass model

Saeed Mahdaviifar

Department of Physics, University of Guilan, 41335-1914, Rasht, Iran

(Dated: July 12, 2018)

The ground state magnetic phase diagram of the one-dimensional quantum compass model (QCM) is studied using the numerical Lanczos method. A detailed numerical analysis of the low energy excitation spectrum is presented. The energy gap and the spin-spin correlation functions are calculated for finite chains. Two kind of the magnetic long-range orders, the Néel and a type of the stripe-antiferromagnet, in the ground state phase diagram are identified. Based on the numerical analysis, the first and second order quantum phase transitions in the ground state phase diagram are identified.

PACS numbers: 75.10.Jm Quantized spin models; 75.10.Pq Spin chain models

I. INTRODUCTION

A theoretical understanding of the magnetic properties of low-dimensional quantum magnets has attracted a lot of interest in the last decades. Especially, ground state properties are interesting since the quantum fluctuation often plays the dominant role at zero temperature. Recently, theoretical works are focused on the important role played by the orbital degree of freedom in determining the magnetic properties of materials. The complex interplay among the spin and orbital degrees of freedom in quantum magnets, such as Dzyaloshinskii-Moriya (DM) interaction^{1,2}, makes their phase diagram rich and induces various fascinating physical phenomena.

The experimental observations on Mott insulators are a realization of the effect of the orbital degrees of freedom on the low-energy behavior of a system. A good candidate for explaining the low-temperature behavior of some Mott insulators is the quantum compass model (QCM)³. In this model, the orbital degrees of freedom are represented by (pseudo)spin-1/2 operators and coupled anisotropically in such a way to mimic the competition between orbital ordering in different directions. The two-dimensional QCM is introduced as a realistic model to generate protected qubits⁴ and can play a role in the quantum information theory. This model is dual to studied model of superconducting arrays⁵. It was shown that the eigenstates are two-fold degenerate and to be gapped⁴. The results from both spin wave study and exact diagonalization have suggested a first-order quantum phase transition in the ground state phase diagram⁶. Recently, the existing of the first-order phase transition is confirmed in two-dimensional QCM^{7,8}. The dilution effect is studied by means of the quantum Monte-Carlo method⁹. It is found that due to dilution, the ordering temperature decreases much stronger than that in spin models. A numerical monte carlo simulation also is done on the square lattice and critical temperatures are obtained for the classical and quantum versions¹⁰.

The one-dimensional (1D) QCM has been studied much less¹¹⁻¹⁶. The Hamiltonian of the 1D QCM on

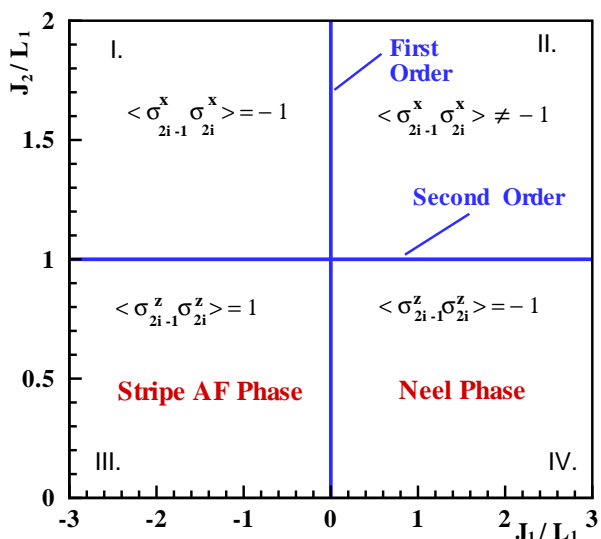


FIG. 1: (Color online.) The phase diagram of the one-dimensional quantum compass model. The first-order and the second-order critical lines denote with $J_1/L_1 = 0$ and $J_2/L_1 = 1$, respectively. The short-range correlation functions in different regions are given by $\langle \sigma_{2i-1}^{x(z)} \sigma_{2i}^{x(z)} \rangle$. In the regions III. and IV., there are the stripe AF and Néel long-range orders, respectively.

a periodic chain of N sites is given by¹⁶

$$\mathcal{H} = \sum_{i=1}^{N/2} J_1 \sigma_{2i-1}^z \sigma_{2i}^z + J_2 \sigma_{2i-1}^x \sigma_{2i}^x + L_1 \sigma_{2i}^z \sigma_{2i+1}^z. \quad (1)$$

Here $\sigma_i^{x,z}$ are the Pauli operators on the i th site and J_1, J_2, L_1 are the exchange couplings. By mapping the model to a quantum Ising model, an exact solution is obtained for the ground state energy and the complete excitation spectrum¹¹. It is shown that the 1D QCM exhibits a first-order phase transition at $J_1 = 0$ between two disordered phases with opposite signs of certain local spin correlations. The degeneracy of the ground state energy

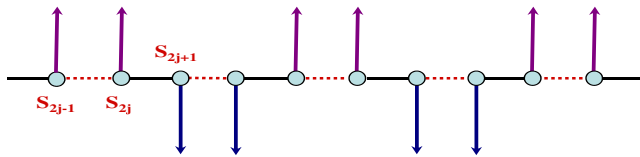


FIG. 2: (Color online.) The Schematic picture of the canted spins in the direction of the z axis, which is known as the saturated stripe-antiferromagnetic order.

at this transition point is $2 \times 2^{N/2}$ in the limit of $N \rightarrow \infty$ and the energy gap is closed. The model is also diagonalized exactly by a direct Jordan-Wigner transformation¹³. The obtained results by latter approach, confirm the existence of the first-order phase transition in the ground state phase diagram. In a very recent paper, Eriksson et.al.,¹⁶ have shown that the reported first-order phase transition, in fact occurs at a multicritical point where a line of the first-order transition ($J_1/L_1 = 0$) meets with a line of the second-order ($J_2/L_1 = 1$) transition. Also, there are four gapped phases in the regions: (I.) $J_1/L_1 < 0$, $J_2/L_1 > 1$, (II.) $J_1/L_1 > 0$, $J_2/L_1 > 1$, (III.) $J_1/L_1 < 0$, $J_2/L_1 < 1$, (IV.) $J_1/L_1 > 0$, $J_2/L_1 < 1$ (see Fig.1). Since the spin ordering in different sectors is obtained by study of short-range correlation functions ($\langle \sigma_{2i-1}^{x,z} \sigma_{2i}^{x,z} \rangle$), the complete picture of different long-range orders of the 1D QCM is unclear up to now.

For the first time, in this paper we perform an accurate numerical experiment on the ground state phase diagram of the model. By analyzing the numerical results on finite chains, we draw a clear picture of the different long-range orders in the ground state phase diagram. In particular we apply the Lanczos method to diagonalize numerically finite ($N = 12, 16, 20, 24$) chain systems. Using the exact diagonalization results, we calculate the various spin structure factors. Based on the exact diagonalization results we argue that instead of the analytical suggested Néel order, the stripe-antiferromagnetic long-range order (see Fig.2) exist in the region (III.) $J_1/L_1 < 0$, $J_2/L_1 < 1$ of the ground state phase diagram. We denote by "stripe-antiferromagnetic phase" the phase with the opposite magnetization along the z axis on the odd bonds.

The paper is organized as follows. In the forthcoming section we present numerical results of our exact diagonalization studies of the system. In Section III, we conclude and summarize our results.

II. NUMERICAL RESULTS

In this section, to explore the nature of the spectrum and the quantum phase transition, we used Lanczos method to diagonalize numerically chains with length up to $N = 24$ and different values of the exchanges (a) $J_2/L_1 = 2(1 - J_1/L_1)$, (b) $J_2/L_1 = 1 - J_1/L_1$ and (c) $J_2/L_1 = (1/2)(1 - J_1/L_1)$. The energies of the few lowest

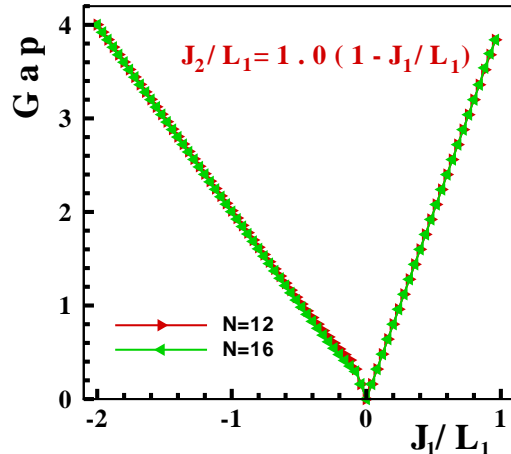


FIG. 3: (Color online.) Difference between the energy of the first excited state and the ground state energy as a function of the exchange J_1 , for chain exchanges $L_1 = 1$, $J_2/L_1 = 1 - J_1/L_1$, including different lengths $N = 12, 16$.

eigenstates were obtained for chains with periodic boundary conditions. The Lanczos method and the related recursion methods^{17,18}, possibly with appropriate implementations, have emerged as one of the most important computational procedures, mainly when a few extreme eigenvalues are desired.

A. The Energy Gap

To show that the transition lines could be observed from the numerical calculations of small systems we start our consideration with the energy gap function. First, we have computed the three lowest energy eigenvalues of chains with different values of the exchanges $J_2/L_1 = 1 - J_1/L_1$. To get the energies of the few lowest eigenstates we consider chains with periodic boundary conditions. In Fig.3, we present results of these calculations for the exchanges $L_1 = 1$, $-2 < J_1/L_1 < 1$ and chain sizes $N = 12, 16$. We define the excitation gap as a gap to the first excited state. As it can be seen in Fig.3, in the considered limit of exchanges, this difference is characterized by the indistinguishable (within the used numerical accuracy) dependence on the chain length and shows an universal linear decrease with increasing exchange J_1/L_1 . At $J_1/L_1 = -2$ the spectrum model is gapped. By increasing the exchange J_1/L_1 from -2 , the energy gap decreases linearly with J_1/L_1 . The energy gap vanishes at $J_1/L_1 = 0$, which is the only level crossing between the ground-state energy and the first excited state energy. With more increasing J_1/L_1 , the spin gap opens again and for a sufficiently large exchange $|J_1/L_1|$, it increases linearly. Therefore, in complete agreement with the analytical results¹⁶, we conclude that in this case, there are two different gapped phases in the re-

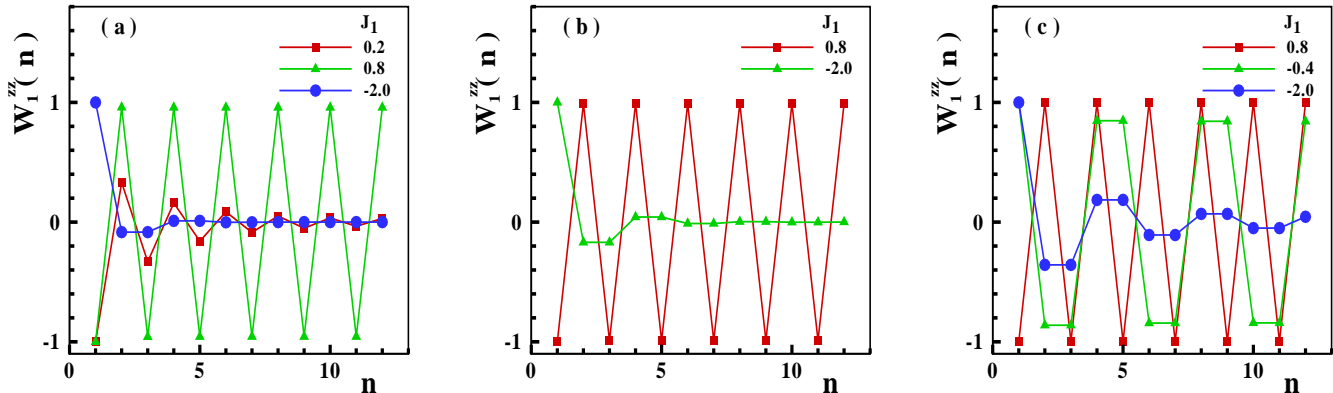


FIG. 4: (Color online.) The spin correlation $W_1^{zz}(n)$ as a function of the n , for chain length $N = 24$ and exchanges $L_1 = 1.0$, (a) $J_2/L_1 = 2(1 - J_1/L_1)$, (b) $J_2/L_1 = 1 - J_1/L_1$ and (c) $J_2/L_1 = (1/2)(1 - J_1/L_1)$.

gions (I.) $J_1/L_1 < 0$, $J_2/L_1 > 1$, and (IV.) $J_1/L_1 > 0$, $J_2/L_1 < 1$.

B. The ground state phase diagram

To recognize the different phases induced by the exchanges J_1 and J_2 in the ground state phase diagram of the 1D QCM, we implemented the algorithm for finite-size chains ($N = 12, 16, 20, 24$) to calculate the order parameters and the various spin correlation functions.

Because of two type of links, we have computed two kind of two-point (short-range) correlation functions defined as $\langle \sigma_{2i-1}^{x(z)} \sigma_{2i}^{x(z)} \rangle$, $\langle \sigma_{2i}^{x(z)} \sigma_{2i+1}^{x(z)} \rangle$. Where $\langle \dots \rangle$ denotes the ground state average. In complete agreement with the analytical results¹⁶, found four regimes with different short-range correlations. In the region $J_2/L_1 < 1$, antiparallel ordering of spin z component on even bonds ($\langle \sigma_{2i}^z \sigma_{2i+1}^z \rangle$) is dominated with respect to the antiparallel ordering of spin x component on odd bonds ($\langle \sigma_{2i-1}^x \sigma_{2i}^x \rangle$) in the region $J_2/L_1 > 1$. On the other hand, in the region $J_1/L_1 < 0$ the ground state is in the $s = N/2$ subspace with $\langle \sigma_{2i-1}^z \sigma_{2i}^z \rangle = 1$ and in the region $J_1/L_1 > 0$, is in the $s = 0$ subspace with $\langle \sigma_{2i-1}^z \sigma_{2i}^z \rangle = -1$. Therefore, the first-order quantum phase transition at $J_1/L_1 = 0$ corresponds to the flip sign of the z component of the pair correlation functions of spins on every first bonds ($\langle \sigma_{2i-1}^z \sigma_{2i}^z \rangle$). In following we try to draw a picture of the magnetic long-range ordering of the system in different ground state phases.

To find the long-range magnetic order of the ground state of the system, we start our consideration with the spin-spin correlation function defined by

$$W_j^{\alpha\alpha}(n) = \langle \sigma_j^\alpha \sigma_{j+n}^\alpha \rangle \quad (\alpha = x, z), \quad (2)$$

and the spin structure factor at momentum q defined by

$$S^{\alpha\alpha}(q) = \sum_{n=1}^{N-1} W_j^{\alpha\alpha}(n) \exp(iqn). \quad (3)$$

It is known that the spin structure factor give us a deep insight into the characteristics of the ground state¹⁹. In Fig.4 we have plotted W_1^{zz} as a function of n along the three paths. In the case of $J_2/L_1 = 2(1 - J_1/L_1)$ we expect three different magnetic phases in the ground state phase diagram, indicated at the regions (I.): $J_1/L_1 < 0$, (II.): $0 < J_1/L_1 < 0.5$ and (IV.): $0.5 < J_1/L_1 < 1.0$. In the case of $J_2/L_1 = \frac{1}{2}(1 - J_1/L_1)$, one additional phase is expected in the region (III.): $-1.0 < J_1/L_1 < 0$. The selected values of the exchange J_1/L_1 in the figure cover all regions of the ground state phase diagram. It can be seen from this figure (Fig.4) that the z component of the spins on odd sites are pointed in the same direction with the σ_1^z and others (on even sites) are pointed in opposite direction at $J_1/L_1 = 0.8$. This is an indication for the Néel ordering in the region (IV.) $J_1/L_1 > 0$, $J_2/L_1 < 1$. It is surprising that the numerical results in Fig.4(c) at $J_1/L_1 = -0.4$ suggest that a different novel phase can exist in the region (III.) $J_1/L_1 < 0$, $J_2/L_1 < 1$. The values of the spin-spin correlation function W_1^{zz} in Fig.4(c) at $J_1/L_1 = -0.4$, show that the two spins on the second odd bond are pointed in the opposite direction with the σ_1^z (or similarly with the two spins on the first odd bond) but two spins on the third odd bond are pointed in the same direction with the σ_1^z . Clearly seen that the mentioned behavior continue in whole of the chain system. We denote this novel kind of the ordering in the ground state magnetic phase diagram of the 1D QCM by the "stripe-antiferromagnetic phase".

Classically, the effect of the negative exchange $J_1/L_1 < 0$ is interesting. In the special case of $J_2/L_1 = 0$, the Hamiltonian reduces to the alternating ZZ Ising model. The ground state of the alternating F-AF ZZ Ising model

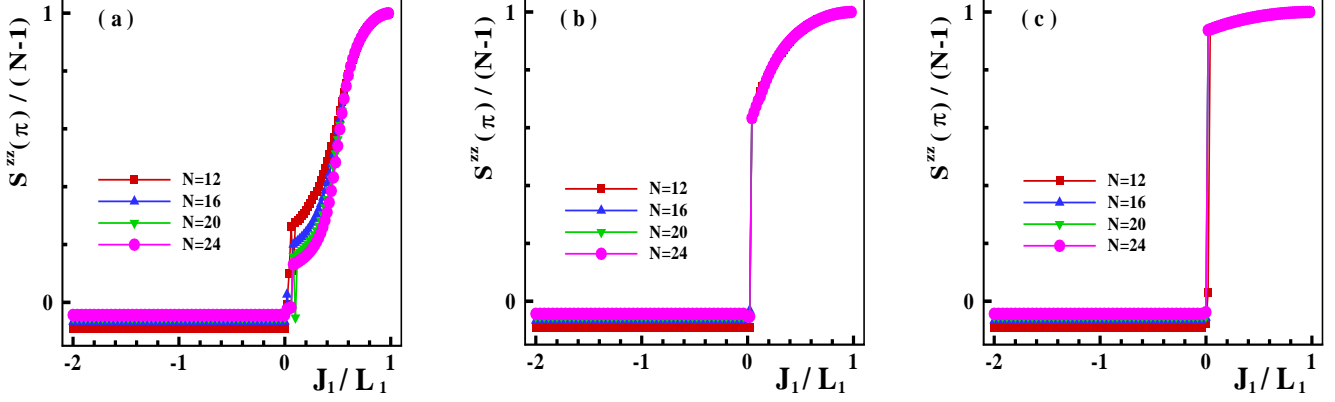


FIG. 5: (Color online.) The spin structure factor $S^{zz}(\pi)$ as a function of J_1 , for chain lengths $N = 12, 16, 20, 24$ and exchanges $L_1 = 1.0$, (a) $J_2/L_1 = 2(1 - J_1/L_1)$, (b) $J_2/L_1 = 1 - J_1/L_1$ and (c) $J_2/L_1 = (1/2)(1 - J_1/L_1)$.

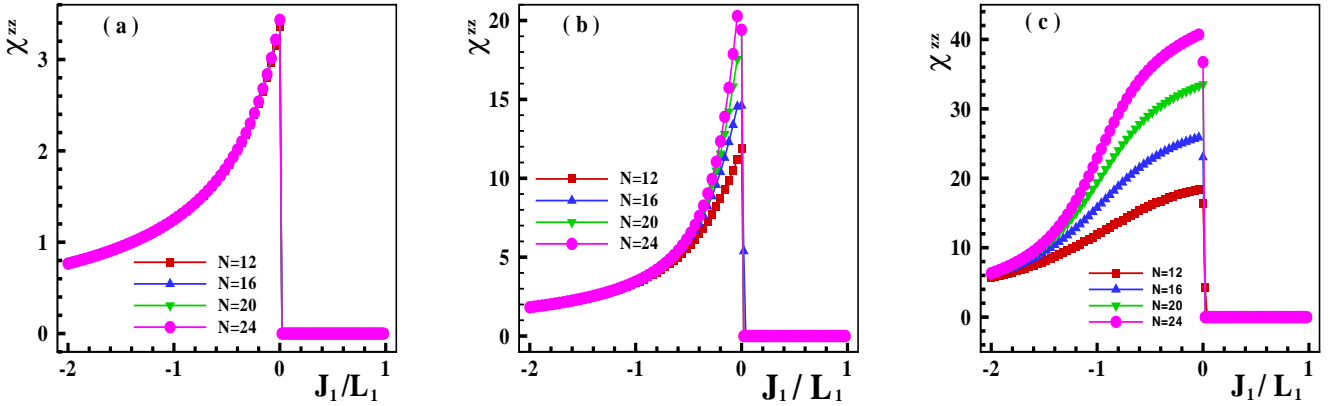


FIG. 6: (Color online.) The correlation function of stripe-antiferromagnetic order χ^{zz} as a function of J_1 , for chain lengths $N = 12, 16, 20, 24$ and exchanges $L_1 = 1.0$, (a) $J_2/L_1 = 2(1 - J_1/L_1)$, (b) $J_2/L_1 = 1 - J_1/L_1$ and (c) $J_2/L_1 = (1/2)(1 - J_1/L_1)$

has a form $|\Psi_{G_s}\rangle = |\uparrow\uparrow\downarrow\downarrow\uparrow\uparrow\downarrow\downarrow\dots\rangle$ with the long-range order canted spins in the direction of the z axis, as illustrated in Fig.2. The ordering of this phase is a type of the stripe-antiferromagnetic phase. Therefore, the order parameter of the stripe-antiferromagnetic phase is defined as²⁰

$$M_{sp}^z = \frac{2}{N} \left\langle \sum_{j=1}^{N/2} (-1)^j (\sigma_{2j-1}^z + \sigma_{2j}^z) \right\rangle. \quad (4)$$

For any value of the J_1/L_1 , the Lanczos results lead to the staggered magnetization, $M_{st}^z = \frac{1}{N} \sum_{j=1}^N (-1)^j \sigma_j^z = 0$, and $M_{sp}^z = 0$, since the ground state is degenerate and in a finite system no symmetry breaking happens. However the spin-spin correlation function diverge in the ordered phase as $N \rightarrow \infty$. We computed the spin structure factor $S^{zz}(\pi)$ and the correlation function of the stripe-

antiferromagnetic order parameter given by

$$\chi^{zz} = \left\langle \sum_{n=1}^{N/2-1} (-1)^n (\sigma_{2j-1}^z + \sigma_{2j}^z) (\sigma_{2j-1+2n}^z + \sigma_{2j+2n}^z) \right\rangle. \quad (5)$$

In Fig.5, we have plotted $S^{zz}(q = \pi)/(N-1)$ as a function of J_1/L_1 for the chain lengths $N = 12, 16, 20, 24$. The J_1/L_1 -dependency of the spin structure factor, $S^{zz}(q = \pi)$, is qualitatively the same as the staggered magnetization, M_{st}^z . It can be seen that in the region (IV.) $J_1/L_1 > 0$, $J_2/L_1 < 1$, the ground state of the system is in the Néel phase. At $J_1/L_1 = 1.0$ (or $J_2/L_1 = 0$), the saturated Néel phase is dominated in well agreement with the zz Ising model. Induced quantum fluctuations by increasing J_2/L_1 from zero (or decreasing J_1/L_1 from the value one), decreases the staggered magnetization from saturation value. In all cases it is clearly seen that the staggered magnetization as a function of the J_1/L_1 , displays a jump to zero at the critical value

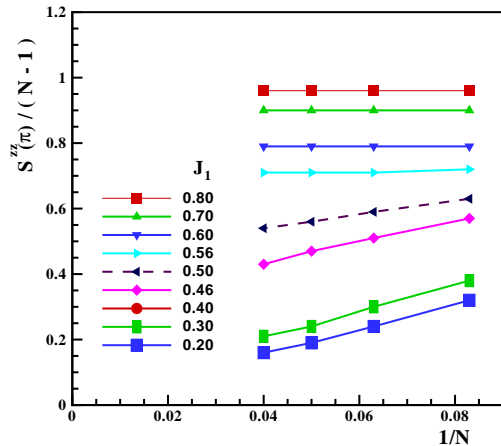


FIG. 7: (Color online.) The spin structure factor $S^{zz}(\pi)$ for $L_1 = 1.0$ and $J_2/L_1 = 2(1 - J_1/L_1)$ plotted as a function of the inverse chain length $1/N$ for different values of the exchange J_1 . The dashed line which correspond to $J_1 = 0.5$ and $J_2 = 1.0$ marks the second order quantum phase transition.

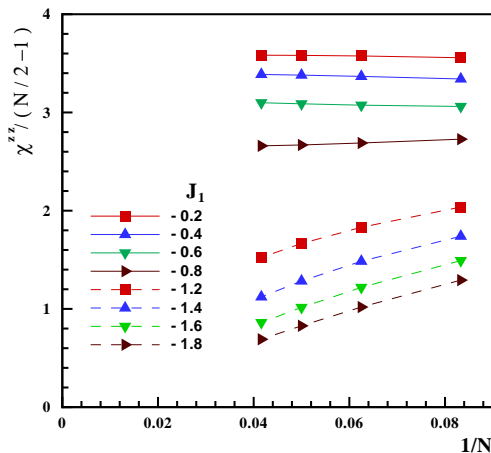


FIG. 8: (Color online.) The correlation function of the stripe-antiferromagnetic order parameter χ^{zz} for $L_1 = 1.0$ and $J_2/L_1 = 1/2(1 - J_1/L_1)$ plotted as a function of the inverse chain length $1/N$ for different values of the exchange $J_1 < 0$. The diminishing behavior of the numerical results (dashed lines) in the region (I.): $J_1/L_1 < -1$, $J_2/L_1 > 1$, shows that the stripe-antiferromagnetic order in the region (I.) is not true long-range (local ordering).

$J_1/L_1 = 0$ which is known as the first-order phase transition. There is not the Néel ordering along z axis in the region $J_1/L_1 < 0$. Overlapping of the numerical results in all regions, except the region $0 < J_1/L_1 \leq 0.5$ and $J_2/L_1 > 1$ (Fig.5(a)), shows a divergent behavior of the function $S^{zz}(\pi)$ by increasing the size of chain N . This justifies that the Néel ordering along the z axis is true

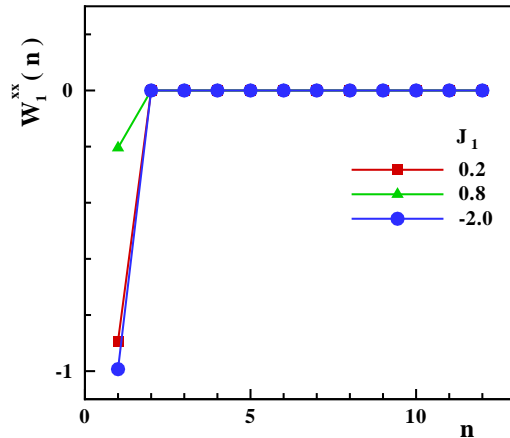


FIG. 9: (Color online.) The spin-spin correlation $W_1^{xx}(n)$ as a function of the n , for chain length $N = 24$ and exchanges $L_1 = 1.0$ and path $J_2/L_1 = 2(1 - J_1/L_1)$.

long-range order in the region (IV.) of the ground state phase diagram. To check the existence of the Néel order in the thermodynamic limit $N \rightarrow \infty$ of the system in the region (II.): $0 < J_1/L_1 \leq 0.5$, $J_2/L_1 > 1$, we have plotted in Fig.7 the N dependence of $S^{zz}(\pi)/(N - 1)$ for different values of $J_1/L_1 > 0$. As is seen from this figure in the region $0 < J_1/L_1 \leq 0.5$, $J_2/L_1 > 1$ there is a diminishing behavior which shows that the Néel order in the region (II.) is local (see also Fig.4(a)). Therefore, we conclude that the Néel order, only exist in the region (IV.) of the ground state phase diagram and a second-order quantum phase transition happens at critical value $J_2/L_1 = 1.0$.

An additional insight into the nature of different phases can be obtained by studying the correlation function χ^{zz} . In Fig.6, we have plotted χ^{zz} as a function of the exchange J_1/L_1 for different values of the chain length $N = 12, 16, 20, 24$. In all cases it is clearly seen that there is no stripe-antiferromagnetic ordering along the z axis in the region $J_1/L_1 > 0$ (regions II. and IV.). In contrast, in the region (III.) $-1 < J_1/L_1 < 0$, $J_2/L_1 < 1$ (see Fig.6(c)), a profound stripe-antiferromagnetic order exist in the z direction. In the limit $J_1/L_1 \rightarrow 0^-$ (or $J_2/L_1 \rightarrow 0.5^+$), by checking the numerical value of the χ^{zz} we found that the saturated stripe-antiferromagnetic phase dominate in the ground state phase diagram. The induced quantum fluctuations by increasing J_2/L_1 from 0.5 (or decreasing J_1/L_1 from zero), decreases the stripe-antiferromagnetic order from saturation value. Also, it is clearly seen that the stripe-antiferromagnetic order displays a jump to zero at the critical value $J_1/L_1 = 0$ which is also an indication of the first-order phase transition. To check the existence of the stripe-antiferromagnetic order in the thermodynamic limit $N \rightarrow \infty$ of the system in the region (III.): $J_1/L_1 < 0$, $J_2/L_1 < 1$, we have plotted in Fig.8 the N dependence of $\chi^{zz}/(N/2 - 1)$

for different values of $J_1/L_1 < 0$. As is seen from this figure in the region $-1.0 < J_1/L_1 < 0$, $J_2/L_1 < 1$ there is a divergent behavior which shows that the stripe-antiferromagnetic order in the region (III.) is true long-range order. On the other hand the diminishing behavior of the numerical results in the region (I.): $J_1/L_1 < -1$, $J_2/L_1 > 1$, shows that the stripe-antiferromagnetic order in the region (I.) is local. Therefore, by investigating the N dependence of $\chi^{zz}/(N/2 - 1)$ for different values of J_1/L_1 , we found that there is no long-range stripe-antiferromagnetic order in regions (I. and II. and IV.) and only long-range stripe-antiferromagnetic order exist in the region (III.). However, the numerical results on finite chains plotted in Fig.6(b), may suggest that there is the stripe-antiferromagnetic long-range order in a very narrow region very close to the multicritical point $J_1/L_1 = 0$, $J_2/L_1 = 1.0$, and at this point jumps from a non-saturate value to zero.

To complete our numerical study of the ground state magnetic phase diagram of the model, we have computed the x component of the spin-spin correlation function W_1^{xx} in all cases. As an example, in Fig.9 we have plotted W_1^{xx} as a function of n along the path $J_2/L_1 = 2.0(1 - J_1/L_1)$. Clearly seen that along the x axis, there are not any conventional magnetic long-range order. We also found the same results for other paths.

III. CONCLUSION

In this paper we have studied the elementary excitation and the magnetic ground state phase diagram of the

1D quantum compass model. We have implemented the Lanczos method to numerically diagonalize finite chains. Using the exact diagonalization results, first we have calculated the energy gap and various short-range correlation functions ($\langle \sigma_{2i-1}^{x(z)} \sigma_{2i}^{x(z)} \rangle$ and $\langle \sigma_{2i}^{x(z)} \sigma_{2i+1}^{x(z)} \rangle$). In complete agreement with analytical results¹⁶, we have showed that there are four regimes with different short-range correlations, which are separated by lines of the first and second-order phase transitions (see Fig.1). Then to answer a very important question: "What are the long-range ordered phases in the ground state phase diagram of the system?", by plotting the spin-spin correlation functions, we have found that two kind of magnetic long-range orders exist in the ground state phase diagram, a type of the stripe-antiferromagnetic and the Néel orders in the regions (III.) $J_1/L_1 < 0$, $J_2/L_1 < 1$ and (IV.) $J_1/L_1 > 0$, $J_2/L_1 < 1$, respectively. By a detailed analysis of the numerical results on the spin structure factors and the correlation function of the stripe-antiferromagnetic order parameter, we have shown that the Néel and the stripe-antiferromagnet orderings are true long-range orders.

IV. ACKNOWLEDGMENTS

Author would like to thank G. I. Japaridze, H. Johannesson, E. Eriksson, H. Sadat Nabi and T. Vekua for very useful comments and interesting discussions.

-
- ¹ I. E. Dzyaloshinskii, J. Phys. Chem. Solids **4**, 241 (1958).
² T. Moriya, Phys. Rev. Lett. **4**, 288 (1960).
³ K. I. Kugel and D. I. Khomskii, Sov. Phys. JETP **37**, 725 (1973).
⁴ B. Douçot, M. V. Feigelman, L. B. Ioffe, and A. S. Ioselevich, Phys. Rev. B **71**, 024505 (2005).
⁵ Z. Nussinov and E. Fradkin, Phys. Rev. B **71**, 195120 (2005).
⁶ J. Dorier, F. Becca, and F. Mila, Phys. Rev. B **72**, 024448 (2005).
⁷ H. -D. Chen, C. Fang, J. Hu, and H. Yao, Phys. Rev. B **75**, 144401 (2007).
⁸ R. Orus, A. C. Doherty, and G. Vidal, Phys. Rev. Lett. **102**, 077203 (2009).
⁹ T. Tanaka and S. Ishihara, Phys. Rev. Lett. **98**, 256402 (2007).
¹⁰ S. Wenzel and W. Janke, Phys. Rev. B **78**, 064402 (2008); Phys. Rev. B **78**, 099902(E) (2008).
¹¹ W. Brzezicki, J. Dziarmaga, and A. M. Oles, Phys. Rev. B **75**, 134415 (2007).
¹² W. -L. You and G. -S. Tian, Phys. Rev. B **78**, 184406 (2008).
¹³ W. Brzezicki, and A. M. Oles, Acta Phys. Pol. A **115**, 162 (2009).
¹⁴ Ke-Wei Sun and Qing-Hu Chen, arXiv:0906.1711.
¹⁵ Ke-Wei Sun, Yu-Yu Zhang, and Qing-Hu Chen, Phys. Rev. B **79**, 104429 (2009).
¹⁶ Erik Eriksson, and Henrik Johannesson, Phys. Rev. B **79**, 224424 (2009).
¹⁷ C. Lanczos, J. Res. Natl Bur. Stand. **45**, 255 (1950).
¹⁸ G. Grosso, L. Martinelli, and G. Pastori Parravicini, Phys. Rev. B **51**, 13033 (1995).
¹⁹ S. Mori, J.-J. Kim and I. Harada, J. Phys. Soc. Jpn **64**, 3409 (1999).
²⁰ S. Mahdaviifar and A. Akbari, J. Phys. Soc. Jpn. **77**, 024710 (2008).